IOP PUBLISHING PHYSICS IN MEDICINE AND BIOLOGY

Phys. Med. Biol. **53** (2008) 4489–4507 doi:10.1088/0031-9155/53/17/002

Efficient Monte Carlo modelling of individual tumour cell propagation for hypoxic head and neck cancer

W Tuckwell[1,2], E Bezak[1,2], E Yeoh[1,3] and L Marcu[1,2]

[1] School of Chemistry and Physics, University of Adelaide, South Australia, Australia
[2] Department of Medical Physics, Royal Adelaide Hospital Cancer Centre, South Australia, Australia
[3] Department of Radiation Oncology, Royal Adelaide Hospital Cancer Centre, South Australia, Australia

E-mail: wendy.tuckwell@health.sa.gov.au

Received 24 April 2008, in final form 16 June 2008
Published 1 August 2008
Online at stacks.iop.org/PMB/53/4489

Abstract

A Monte Carlo tumour model has been developed to simulate tumour cell propagation for head and neck squamous cell carcinoma. The model aims to eventually provide a radiobiological tool for radiation oncology clinicians to plan patient treatment schedules based on properties of the individual tumour. The inclusion of an oxygen distribution amongst the tumour cells enables the model to incorporate hypoxia and other associated parameters, which affect tumour growth. The object oriented program FORTRAN 95 has been used to create the model algorithm, with Monte Carlo methods being employed to randomly assign many of the cell parameters from probability distributions. Hypoxia has been implemented through random assignment of partial oxygen pressure values to individual cells during tumour growth, based on *in vivo* Eppendorf probe experimental data. The accumulation of up to 10 million virtual tumour cells in 15 min of computer running time has been achieved. The stem cell percentage and the degree of hypoxia are the parameters which most influence the final tumour growth rate. For a tumour with a doubling time of 40 days, the final stem cell percentage is approximately 1% of the total cell population. The effect of hypoxia on the tumour growth rate is significant. Using a hypoxia induced cell quiescence limit which affects 50% of cells with and oxygen levels less than 1 mm Hg, the tumour doubling time increases to over 200 days and the time of tumour growth for a clinically detectable tumour (10^9 cells) increases from 3 to 8 years. A biologically plausible Monte Carlo model of hypoxic head and neck squamous cell carcinoma tumour growth has been developed for real time assessment of the effects of multiple biological parameters which impact upon the response of the individual patient to fractionated radiotherapy.

1. Introduction

1.1. Head and neck cancer and hypoxia

Squamous cell carcinoma of the head and neck (HNSCC) describes aggressive, malignant disease affecting sites such as the oral cavity, pharynx, oropharynx, tongue, nasopharynx and oesophagus. Cancers of the head and neck account for approximately 3% of all human malignancies and approximately 500 000 HNSCC are diagnosed world wide each year, with the majority being locally advanced at presentation (Bourhis *et al* 2006). Surgery, radiotherapy and chemotherapy may be used alone or in combination to control the disease, with radiotherapy being the most common form of treatment. Currently, radiotherapy local control rates are approximately 80% for early stage disease, but this becomes significantly lower (often below 50%) for locally advanced tumours. Efforts to improve these statistics through dose and fractionation modifications have been made in recent decades using different radiation dose schedules but the prognosis has not improved significantly (Koukourakis *et al* 2006, Dinshaw *et al* 2006, Stadler *et al* 1998).

Hypoxia, defined as a lack of an adequate supply of oxygen in tissue, occurs commonly in HNSCC and is a significant cause of treatment failure because hypoxic cells are up to 3 times more resistant to radiotherapy (Palcic *et al* 1984, Gray *et al* 1953). From a radiobiological perspective, hypoxia of a cell is said to exist if partial oxygen pressure (pO_2) is 10 mm Hg or less. However, reports from clinical trials often express hypoxia as the percentage of cells in the tumour with pO_2 less than 5 or 2.5 mm Hg. The normal range of pO_2 for healthy epithelial cells may range from 20 to 100 mm Hg with an average of 40–50 mm Hg (Adelstein *et al* 2005, Adam *et al* 1999).

Hypoxia arises in the tumour mass if the oxygen supply is inefficient, which may be due to effects such as the increased demand for oxygen in the rapidly proliferative cell population and the irregular and chaotic nature of tumour vessel networks. Hypoxic regions may be anywhere in the tumour mass but are most commonly observed at the tumour core, which is likely to be located further from functioning blood vessels than at its periphery (chronic hypoxia). Temporary hypoxia (acute hypoxia) may also be observed if there are temporary shortages in blood flow, for reasons such as the fluctuation in mechanical pressures on the tumour.

Approximately 70% of locally advanced head and neck tumours have been shown to have hypoxic regions (Rischin *et al* 2006, Becker *et al* 1998) and there is direct evidence that the hypoxic sub-volume and mean oxygen level have a direct influence on local control of head and neck tumours (Nordsmark *et al* 2005, Dunst *et al* 2003, Stadler *et al* 1998, 1999, Brizel *et al* 1999, Gatenby *et al* 1988). Further, up to 30% difference in time to recurrence and 10% difference in death rates at 5 years has been found in clinical trials when separating patient groups into low and high oxygenation groups (Adam *et al* 1999, Nordsmark *et al* 2005).

A large range in individual patient values for fractional hypoxic volumes within the tumours exists. Furthermore, there is a wide distribution of oxygen levels within a single tumour. These wide variations provide the basis for developing tumour models and treatment planning algorithms based not only on the presence of hypoxia, but also on the individual hypoxic tumour volumes and the oxygen distribution within the tumour. There is considerable evidence in the literature supporting the value of modelling (Dutching and Vogelsaenger 1985, Dionysiou *et al* 2004, Dasu *et al* 2005, Harting *et al* 2007) based oxygen distribution in the tumour and clinical trial data which stratify for hypoxic volumes (Dunst *et al* 2003).

Tumour modelling has the potential for faster and more individualized radiotherapy treatment planning. Modelling allows patient specific biological data to be considered, and

allows for changes in parameter values and ranges to be evaluated for their affects on the entire tumour system. Using Monte Carlo modelling methods, cell based parameter changes can be implemented and their impact analysed by varying macroscopic tumour properties such as: tumour growth rates/doubling times (TD), the percentages of cells differing proliferation potential within the tumour population, the percentage of hypoxic cells and the rate of repopulation and reoxygenation throughout treatment. A cell specific and multi-parameter system such as this would not be feasible using an equation based deterministic method of modelling.

1.2. Research aims

The broad aims of this study are to develop a HNSCC tumour growth computer model to assess the major influences on tumour growth rate on an individual basis. The model should provide a tool for not only growing a tumour much faster than in a living model, but also for analysis and changes to be included any point in time. It should be relatively simple to use, run efficiently in time and memory capacity and have the flexibility to allow further cell based and global parameters to be applied to the model for further developments. It should also have the flexibility to allow for the effect of individual radiotherapy fractionation schedules and different degrees of tumour oxygenation as well as reoxygenation and repopulation during RT.

1.3. Review of the tumour modelling literature

Many groups have undertaken the task of simulating the growth and subsequent treatment of human tumours using mathematical and computer systems. They have done so through various methods which have used either analytical deterministic or stochastic Monte Carlo type approaches. For the more recent models include parameters of constituent tumour cell groups or of individual cells, both methods have been used for an automaton approach to spatially organize and visualize the tumour, or to concentrate purely on the temporal behaviour of the system.

Based on previous work (Gray *et al* 1953) which showed that cells undergoing radiotherapy are more resistant in the absence of oxygen, Thomlinson and Gray (Thomlinson and Gray 1955) first used the theories of simple geometry and diffusion (Hill 1928) to mathematically predict the presence and location of chronic hypoxia of tumour cell cords. Their model was justified by experimental results which revealed no presence of central necrosis in tumour cell cords in squamous cell carcinoma of the bronchus, which were less than 160 μm in diameter. Work by Tannock followed in the late 1960s and early 1970s which went on to describe the radiosensitivity of tumours based on the distribution of tissue oxygenation (Tannock 1968, Tannock and Steel 1970, Tannock 1972).

Two of the earliest groups to describe the tumour system using stochastic methods and individual cell or cell sub-group modelling were led by Donaghey (1980) and Dutching (Dutching and Vogelsaenger 1981, 1985) during the late 1970s and early 1980s. This work led to the progression into the first stochastic tumour population modelling algorithms (Donaghey 1980, Smolle and Stettner *et al* 1993, Qi *et al* 1993) and further into modelling the effects of chronic hypoxia in tumours and how the potential doubling time and hypoxic cell life span impacted on the extent of hypoxic in solid tumour segments (Maseide *et al* 1999). In more recent times, tumour modelling has become more specific in terms of tumour site, cell characteristics and also to include modelling of treatment parameters to a larger extent (Kocher *et al* 2000, Dionysiou *et al* 2004, Borkenstein *et al* 2004, Harting *et al* 2007).

The current model extends upon the work within Department of Medical Physics, developed by Marcu *et al* (2002) at the Royal Adelaide Hospital and IMVS Research Facility. This work analysed the mechanisms and influences of tumour growth kinetics and was extended to consider the temporal aspects of chemotherapy in combination with radiotherapy and their effects on tumour kinetics and treatment outcome. The work in this text contributes to the tumour modelling literature by providing an individual tumour cell propagation model which includes: an epithelial cell proliferative hierarchy, a plausible log-normal distribution of oxygen amongst the individual tumour cells, oxygen and cell type dependent cell cycle times, cell quiescence and radiosensitivity (for future radiotherapy studies). The model algorithm has been written in FORTRAN 95 which has proven to be efficient for the type of coding required in the model, and has been designed to be efficient and flexible for data handling and storage. It may also be readily developed and extended to further investigations into radiotherapy treatment effects on tumour cell kill for well oxygenated or for hypoxic tumours of varying degrees of oxygenation.

2. Methods

2.1. Modelling tumour cell division

2.1.1. Carcinogenesis and cell hierarchy. There are many theories of how genetically mutated cells progress to develop into a malignant tumour. In this work it has been assumed that HNSCC is initiated by a single mutated stem cell. This cell type is typically found in the basal (lower) layer of epithelial tissue (Leary *et al* 1984, Morris *et al* 2004). The cell hierarchy structure used in the model was developed through the information provided by previous stem cell biology and modelling work (Aarnaes *et al* 1990, Wright and Alison 1984, Marcu *et al* 2002).

Stem cells are self renewing cells, and are often also described as being clonogenic, meaning that they divide indefinitely, and they are responsible for maintaining the integrity of the epithelial tissue by boosting the cell population. Stem cells may be in a proliferative (dividing) or quiescent state. In the lower and intermediate layers of the epithelium, cells with limited proliferative capacity exist, called transit cells. These cells may undergo a finite number of divisions, producing more transit cells or differentiating cells (post-mitotic cells). In the higher layers, cells more specialized and eventually become fully differentiated. Fully differentiated cells are eventually lost through natural cell death processes and replaced through cell division from the layers below. Epithelial tissue of the structures of the head and neck is primarily non-keratinizing (does not form the protein keratin, unlike skin), but like skin it is also stratified, as shown in figure 1.

2.1.2. Cell type definitions programmed cell division structure. Although the layered structure of normal epithelial tissue may be distorted in tumouros tissue, it has been assumed in the model that the percentages of different cell types are approximately maintained. This assumption is made on the premise that the HNSCC tumour system is one in which the balance between cell production and cell loss no longer exists, although it retains cells of a wide range of proliferative capacities (which may vary depending on tumour differentiation status).

In the model, a dividing stem cell always produces at least one daughter stem cell (a property of self renewing stem cells), and the second daughter cell is either another stem cell, a first generation 'transit' cell ('T1') or a differentiating cell ('D1', a differentiating cell that would in healthy tissue be located in the basal layer). Stem cells may be in a quiescent or

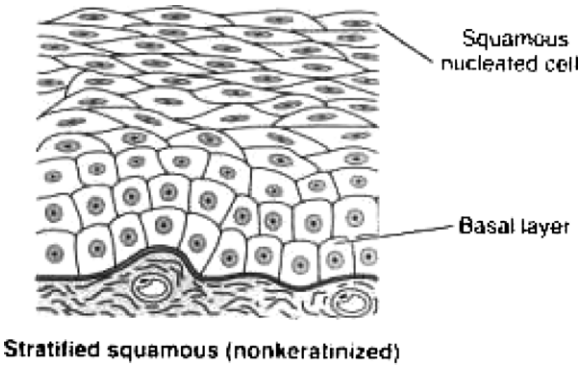

Figure 1. Epithelial non-keratinized stratified squamous cell structure (Henrikson *et al* 1997).

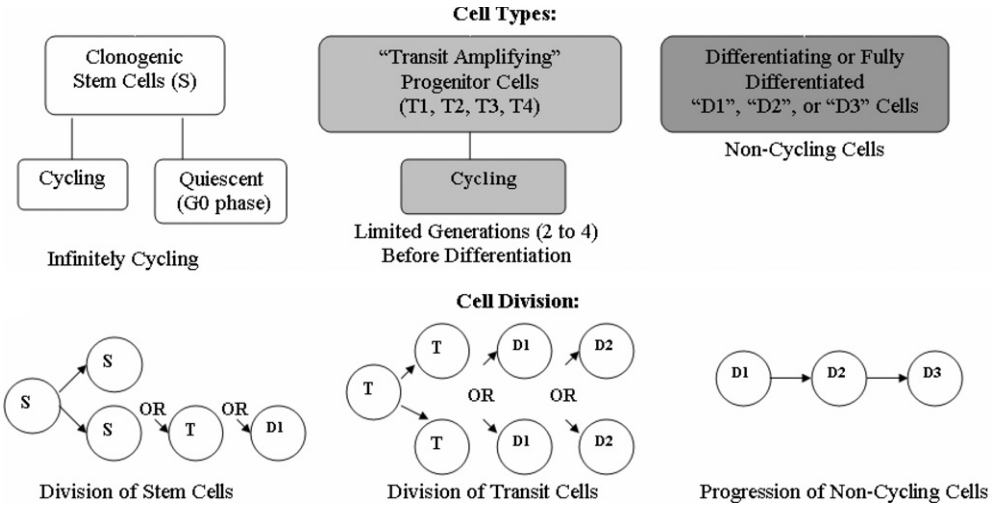

Figure 2. Epithelial cell proliferative hierarchy used in the model. The diagram shows the different cell types modelled and their potential cell daughter products upon division.

cycling state. The ratio of the probabilities for the cell type of the second daughter cell is called the 'S:T1:D1' ratio.

The modelled transit cells divide into two daughter transit cells, until a predefined generation number (between 1 and 4) has been reached (generation number is described as 'T1' for first generation, 'T2' for second generation etc), at which time the last generation transit cell divides in to two differentiating cells ('D1' or 'D2').

The modelled differentiating cells go through three phases before cell death, the 'D1', 'D2' and 'D3' phases. The 'D1', 'D2' phase cells are produced from stem or transit cell divisions. Both the 'D1' and 'D2' cells progress into the 'D3' phase. 'D3' cells are those cells which have become fully differentiated and exist for a finite period before being lost to natural cell death processes (Wright and Alison 1984, Aarnaes *et al* 1990, 1993). See figure 2 for a diagram cell types and division products applied in the model.

The primary difference between the healthy tissue and the modelled tumour tissue is the increased probability of stem cell division where two daughter stem cells are produced. This probability is called the stem cell symmetrical division probability and will be referred to as S% (also as 'S' in the S:T1:D1 ratio).

Daughter cell products upon division of the various cell types have been determined in the model based on literature data of the cell type percentages in the total cell population likely to be present in normal epithelial tissue and therefore also in their malignant counterparts (Aarnaes *et al* 1990, Wright and Alison 1984, Steel 2002, Appleton *et al* 2002, Marcu *et al* 2002). Aarnaes *et al* took great detail in mathematically and experimentally exploring the percentages of proliferating and quiescent cells in the basal layer of the epithelium, as well as the different cell cycle and phase durations in cells at different times of the day. The latter parameter does not form part of the current study, although it merits consideration at a later date owing to the impact on the redistribution of cells in the cell cycle during fractionated radiotherapy.

A 12%–50% D1 population amongst the basal layer cells and an approximate 50% proliferating population in the basal layer has been reported (Aarnaes *et al* 1990). This group has also estimated the percentage of cells in the G0/G1 phase awaiting migration to be approximately 20% in the basal layer. The total non-cycling population was assumed to be 80%–90% of the total cell population, and that the differentiated group of cells had a high probability of cell death (apoptotic and other natural death processes). These data were noted while adjusting parameters so that the final cell type percentages were in plausible ranges (results presented in section 3.1).

The approach of modelling the cells which do impact significantly on tumour growth rate, more accurately reflects the biology and cell type percentages that have been previously reported (Aarnaes *et al* 1990, Wright and Alison 1984, Marcu *et al* 2002). Consequently, effects of parameter values and ranges on the cell populations have been made simpler to analyse in terms of impact upon the cell type percentages.

It should be noted that no DNA or gene mutation information is modelled in this work and only tumour cells (no normal tissue) have been considered. The model does not take into account any spatial information about the cells, i.e., no specific layered structure, as temporal information only is retained for each cell.

2.2. Monte Carlo modelling approach

2.2.1. Stochastic modelling technique and programming language. Monte Carlo modelling techniques were employed so that multiple biological parameters could be considered simultaneously, since many parameters involve the use of probability functions. The program has been written in the FORTRAN 95 programming language and used in the Microsoft Visual Studio 2003 environment. This language was chosen for this project because of the computational speed achievable through the use of basic functions and commands. Early in development, the program was written in the MATLAB programming language and compared in terms of computational speed, using similar basic functions and a programming style. The use of MATLAB showed more than a five fold decrease in computational efficiency.

The simulations that have produced the results in section 3 have used a total cell population of 10^7 cells. This number was chosen to limit the time taken to produce the required results, whilst acquiring a sufficient cell population to model the initiation of tumour hypoxia (10^6 cells). Note that the variations in model in terms of the cell population percentages and tumour growth rates are negligible at this cell number, considering the fluctuations caused by altering the random number seed.

2.2.2. Algorithm design. The 95 edition of FORTRAN 95 has the advantage of being 'object oriented'. Each cell in the tumour model is declared as an object. Each object may have many attributes assigned to it, each with a different numerical precision if required. For the model in its current state, there are five such attributes stored as integers, in one 4-byte and three 1-byte words. These attributes include: the cell type, generation number, cell cycling time, time at which the cell is due to divide, and the oxygenation level.

The storage of cell data and data handling is structured using a large two-dimensional array of cells. Each element in the array houses one cell or 'object'. The algorithm is designed such that as each cell divides, two new daughter cells emerge and the mother cell ceases to exist. The two new cells are allocated their respective attributes and stored within the array. Each row in the array houses a stack of cells and represents one hour of time (relative to the tumour), i.e., cells which are due to divide within a certain hour are stored in the same stack and remain there until the stack is due to divide. This is an efficient way of organizing the cell data storage and for reading and writing data to computer memory.

The cell division algorithm was designed such that cells divide in chronological order according to their assigned cell cycle time (CCT), followed by multiple parameter assignment to the daughter cell products. All individual cell attributes in the growth model are allocated upon creation of the cell and remain fixed through out its lifetime; however, one daughter cell retains the mother cell oxygenation level, as it effectively replaces the position that the mother cell used to reside. The second daughter cell will have a new oxygen value randomly allocated from a probability distribution.

Stacks of cells are divided in chronological order, at which time daughter cells are created and immediately stored in a new stack, corresponding to their allocated Cell Cycle Time (CCT) and the current tumour time. There are 59 stacks in the array (maximum CCT = 59 h), and when the current tumour time is 60 h or greater the array starts to have the stacks recycled. See figure 3 for a flow chart of the cell division algorithm.

2.2.3. Modelled parameters. Many biological parameters are included in the model. These are based on the literature average values wherever possible. These parameters include: the distribution of values for CCT, necrotic cell death rates, cell repair probabilities, stem cell symmetrical division probability etc. Quantitative values of some parameters are yet to be identified experimentally, and consequently have been applied in the model through estimated values or probability distributions. The applied parameters were then analysed for global effects over a wide but reasonable range of values. See table 1 for parameter values and references.

2.2.4. Algorithm efficiency. Care was taken to design the cell division algorithm with a high computational efficiency. This meant designing the program code at a basic code level, with a minimum number of modules and pointers to in-built functions. The method of using a two-dimensional array (where each column stores cells that are due to divide within the same hour of tumour time) to store cell data, was the most efficient way to store, access and manipulate data as the modelled cells divide, die and accumulate in the program. Other methods were explored (using other programming package, and using other linear vector approaches), but alternative methods either created more data to store or were slower in their processing times.

2.3. Modelling hypoxia

2.3.1. The modelled tumour oxygen distribution. A lognormal distribution has been fitted to literature data of pO_2 versus frequency of measurement (histogram) from Eppendorf probe

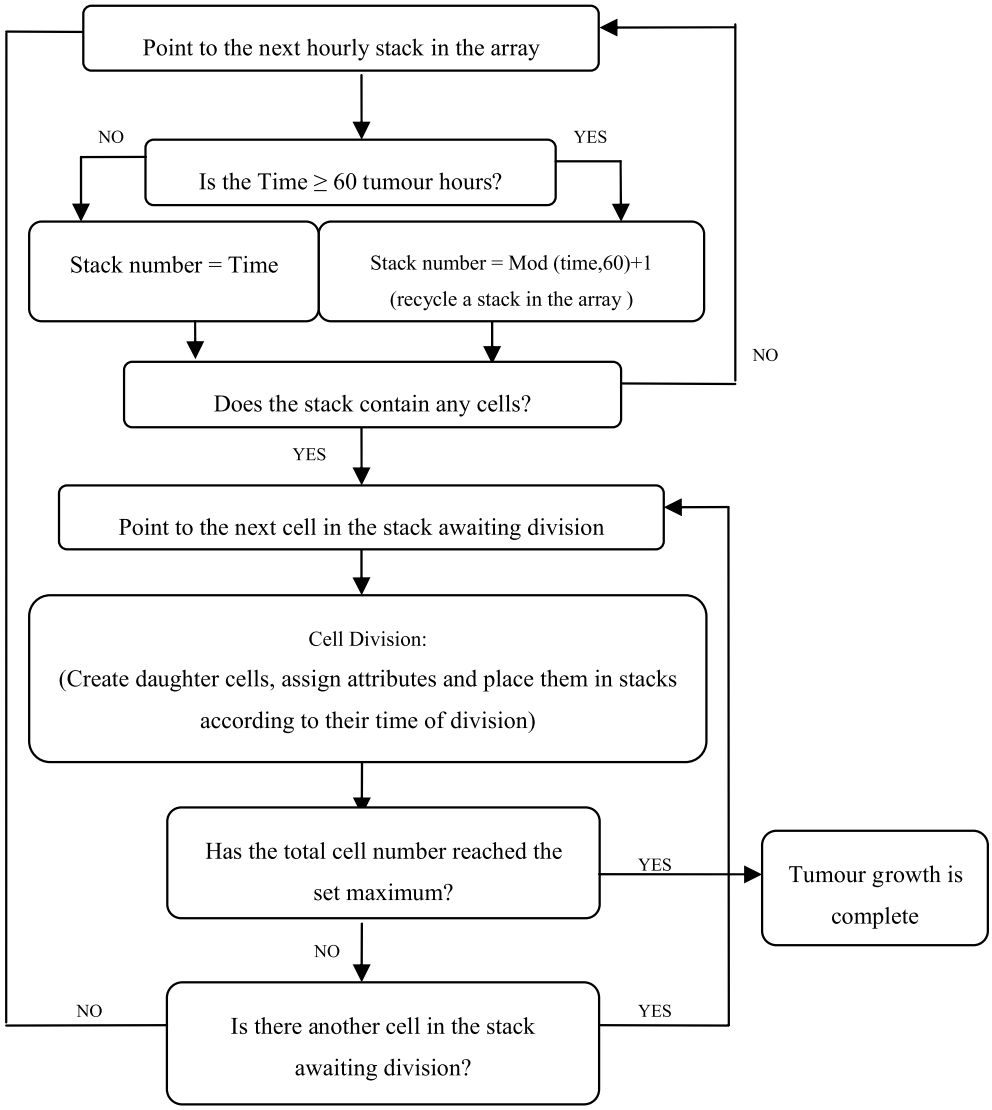

Figure 3. Cell division algorithm flow chart, where all references to time and in terms of time relative to the tumour, in hours, and not the running time of the program.

data in clinical trials (Lartigau *et al* 1998, Adam *et al* 1999), as shown in figure 4. This distribution is used in the Monte Carlo code which randomly assigns each cell a pO_2 value. As previously mentioned, as a cell divides one daughter cell receives the mother cell pO_2 level and the other daughter cell receives a value taken from the distribution shown in figure 4. To avoid a bias, the mother cell pO_2 level has an equal chance of being passed on to the first or second daughter cell.

2.3.2. Assigning of oxygen levels to the cell population. The method of assigning oxygen levels to each cell from a set probability distribution is in contrast to other models which tend

Table 1. Key parameters in the growth model including the parameter value, range, distribution and literature references.

Parameters	Value used in the model	Range	Reference	Comments
G0 stem phase duration	5 h	Exponential, mean = 5 h	Izquierdo and Gibbs 1972 Indirect: Wright and Alison 1984, Potten *et al* 1986, Hill and Tannock 1998	Total average CCT (G0 and cycling phases) is ∼33 h, with a small number of cells remaining in G0 for a relatively long time
Cell cycle time (stem cell)	27 h	Gaussian, sigma = 3 h	Indirect: Wilson *et al* 1988, Hill and Tannock 1998, Begg *et al* 1999, Steel 2002, Mantel *et al* 2001	The G0 phase adds to the length of time before stem cell division
Cell cycle time (transit cell)	33 h	Gaussian, sigma = 6 h		With 2 to 4 generations of division
Differentiating Time: D1 & D2 cells	D1: 36 h D2: 36 h	Uniform: range of 24–48 h	Indirect: Wright and Alison 1984, Potten 1997	Estimate based on 1–2 week cell turnover in epithelial tissue based on 3 transit cell divisions
Fully differentiated 'D3' cell natural death rate	D3: 80%	Constant	Indirect: Steel 2003 (∼85% cell loss factor)	This cell loss rate for the fully differentiated cells means that the total aver age cell loss is ∼85% for the whole population where TD ∼ 40–45 days
Stem cell division products i.e. the S:T1:D1 ratio	S = 3% T = 87% D1 = 10%	Constant	Steel 2003	This ratio produces an approximate 1% stem cell population in the tumour
Oxygen distribution	5 mm Hg	Log-normal	Lartigau *et al* 1998, Adam *et al* 1999, Hall 2005	A log-normal describes the literature data using Eppendorf electrodes. Values range between 1 and 100 mm Hg
Spontaneous death of D1 & D2 cells upon mother cell division	D1: 10% D2: 10%	Constant	Steel 1997	Aging and spontaneous apoptotic death considered
Transit cell division probability	D1: 80 D2: 20	Constant	Aarnaes *et al* 1990	
Low oxygen limit for cell cycle arrest	1 mm Hg	Constant	Indirect: Alarcon *et al* 2004, Ljungkvist *et al* 2002	
Hypoxic cell half life (the time after which, half of the extremely hypoxic cells are programmed to die due to necrosis: $pO_2 < 1$ to 2 mm Hg)	4 days	Constant	Durand and Sham 1998 Ljungkvist *et al* 2005	4 to 10 day hypoxic cell lifetime in human colon carcinoma spheroids 2 days in xenograft HNSCC

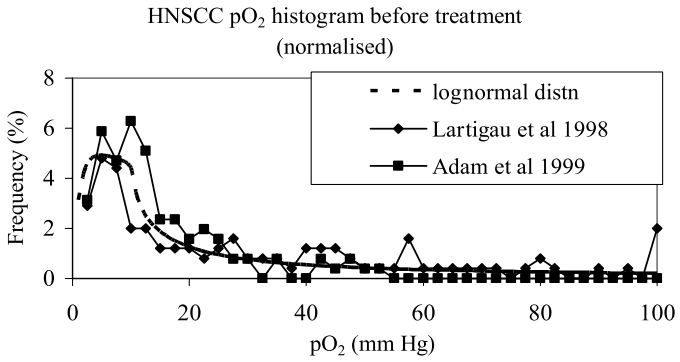

Figure 4. pO_2 histogram data measured using the Eppendorf electrode technique.

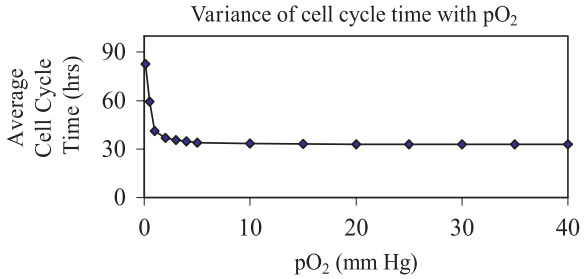

Figure 5. Slowing of the cell cycle with pO_2 (mm Hg), theory adapted from information from Alarcon *et al* (2004) and fitted to an exponential curve using the formula $f = y_0 + a * \exp(-b * x)$, where $y_0 = 33.27$, $a = 58.88$, $b = 1.73$, $r^2 = 0.993$.

to use diffusion distances from uniformly spaced capillary cells (Borkenstein *et al* 2004, Dasu *et al* 2005, McElwain *et al* 1979), or oxygen levels based on radial distances. The method has the benefits of being flexible, in that it can be easily interchanged for different oxygen data sets and because it can be changed during the growth period (or treatment) if required for a single simulation. It is also a simple and randomized method of assigning each cell an oxygen value, which is reasonable due to the spatial and temporal irregularity of hypoxia in advanced *in vivo* tumour systems (Ljungkvist *et al* 2002).

Further, many models do not consider the range of oxygen levels which may lie between 0 and 100 mm Hg. The range is important due to the slowing of the cell cycle with decrease in the oxygen levels (Alarcon *et al* 2004, Ljungkvist *et al* 2002, Wilson *et al* 1995, Gardner *et al* 2001, Hirst and Denekamp 1979). In the model, a threshold for cell cycle arrest was applied for cells with very low oxygenation, as cells cannot survive in extreme hypoxic conditions and eventually die of necrosis, after arrest in the G1 phase of the cell cycle (Koritzinsky *et al* 2001).

This threshold value was varied and the results analysed. Cells with oxygen levels above this threshold had their allocated cell cycle time increased by a factor between 1 and 3, according to the modelling work of Alarcon *et al* (2004) (figure 5). Cells with oxygen levels below the threshold become quiescent and are programmed to die, using a half life parameter. This parameter is modelled so that half of the hypoxic quiescent cells die at regular intervals. This means that hypoxic quiescent cells do not need their entire attribute data stored, rather a

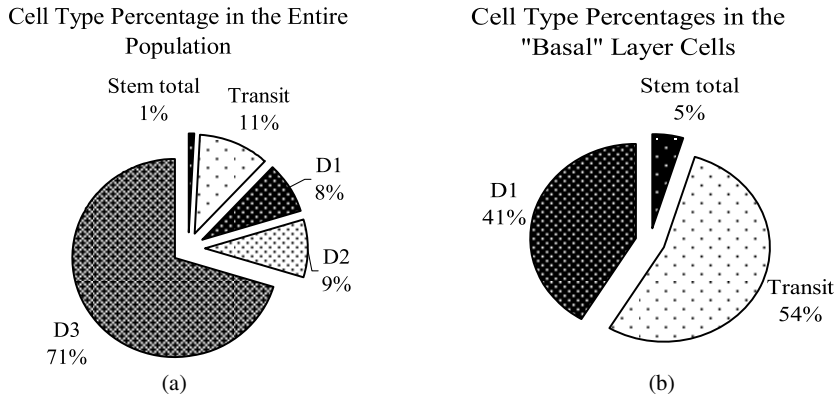

Figure 6. The percentages of cells of different proliferative hierarchy arising in the model (a) in the total cell population, and (b) of cells that would normally reside in the basal layer of the epithelium.

single counter parameter which counts the total number of cells can be utilized. This counter then reduces to half at the predetermined regular interval desired.

3. Results and discussion

3.1. Cell division and tumour growth properties

3.1.1. Percentages of different cell types in the cell population. As mentioned in the previous section, normal epithelial tissue consists of a small percentage of stem cells, transit cells, differentiating cells and fully differentiated cells in the cell population. Assuming a relatively close relationship between these percentages in normal tissue compared to tumour tissue, the following cell type percentages resulted in the model, using the parameters displayed in table 1, and as seen in figures 6(a) and (b).

3.1.2. Influence of symmetrical stem cell division probability on tumour growth. The results which follow show the influence of the symmetrical stem cell division probability on the tumour growth rate, tumour doubling times, total tumour growth times and the cell type percentages in the population.

An increase in the symmetrical stem cell division probability (S%) parameter, has a major effect on the tumour growth curve, the total tumour growth time and the tumour doubling times. Altering the S% parameter to values between 1% and 5% resulted in a reduction in average tumour doubling times ranging from 116 to 23 days (figure 7).

Average tumour doubling times were calculated using total cell numbers which were recorded every 100 h, which were then averaged over the last 1000 h of tumour growth. Large fluctuations in the tumour doubling time are evident until approximately 1 year of tumour growth and may account for a 100 or more day difference in initial compared to the final tumour doubling times. The inverse relationship between tumour doubling time and total growth times with S% are shown in figures 8 and 9.

The choice for 'S%' of 3%, resulted in average tumour doubling times of approximately 40 ± 1 day in the model, which is consistent with the ranges reported in the literature of for head and neck squamous cell carcinomas (40–45 days, Steel (2002) and Denham (2001)).

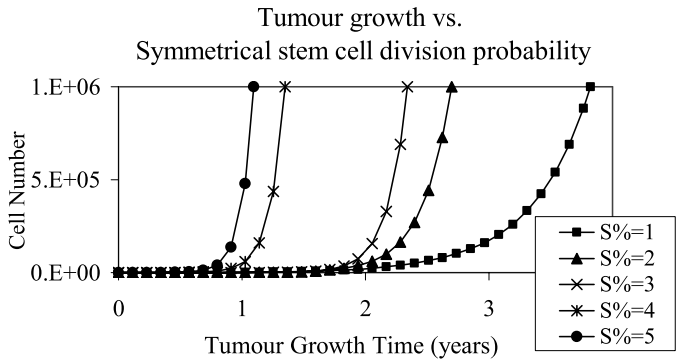

Figure 7. Cell growth curves for various symmetrical stem cell division probabilities.

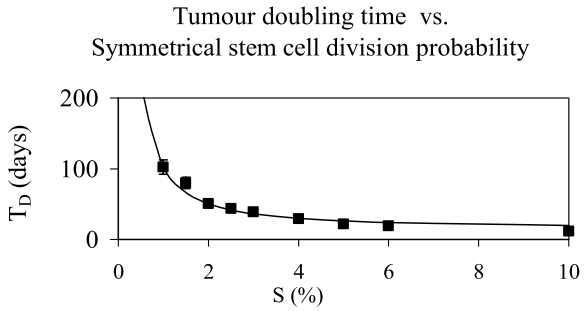

Figure 8. The influence of the stem cell symmetrical division probability on tumour doubling time.

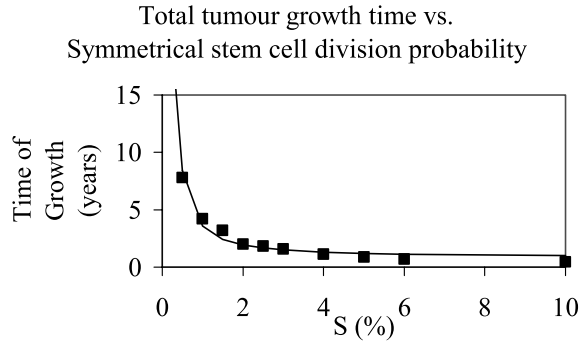

Figure 9. The relationship between the symmetrical stem cell division probability and time (10^6 cells) with all cells in the model fully oxygenated.

A doubling time close to the lower doubling times reported in the literature was chosen because of the fully oxygenated state of the tumour during these simulations.

It is well known that when hypoxia begins to impact upon tumour growth, the doubling time will correspondingly increase, and as the majority of head and neck cancers have some hypoxic areas present at diagnosis, the true oxic tumour doubling time is likely to be even

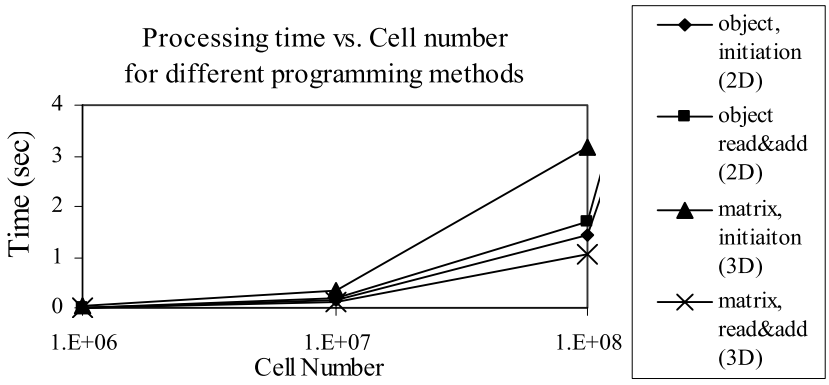

Figure 10. An example of the processing time (array initialization and reading/writing to array elements) for the 2D object array versus 3D array data storage techniques, during model development.

smaller than presented here. In any case, a wide variation in growth rates among patients has been observed, and ideally a parameter set applicable to the individual patient should be used in the model (along with consideration of the current oxygenation status and tumour size).

3.2. Impact of the algorithm design

3.2.1. Variations in tumour growth due to random number seed. The tumour growth program was run for many different random number seeds. Regardless of the choice of seed, the tumour doubling time settled to approximately 40–45 days, or 1.07 growth rate per 100 h (comparable to results reported by Marcu *et al* (2002)) in all cases after 1.5 years of simulated tumour growth with all seeds having similar amplitude fluctuations. Relatively large fluctuations in the early stages of growth occur for most random seed choices, and were due to the small cell numbers and therefore increased variance in the number of stem cells in the early population.

3.2.2. Algorithm efficiency. A two-dimensional (2D) array method for cell data storage was compared for computation efficiency to a three-dimensional (3D) array approach. The difference between to the two methods involves the use of 'objects' versus vectors to store cell attribute data. In the 2D case, a single array was used, where each cell or 'object' contained integer numbers. In the 3D case, an array of the same dimensions was declared, with the third dimension equal to 3 array elements. Here, each element is stored as a single integer value.

Early in the model development (3 attributes per cell modelled only) array initialization and read/write times were analysed, as shown in figure 10. Overall, the 2D object array method was faster to process predominantly due to the large initialization time required for the 3D array method. The difference between reading and writing data from either a 2D object array or a 3D array was insignificant. The 3D approach had the disadvantage of requiring each element to have the same numerical precision, which was a waste of computer memory for those attributes requiring less than the standard single precision integers or real numbers (4-bytes). Currently, up to 10^7 cells may be propagated in ten to fifteen minutes on a standard PC using the 2D object approach to data storage, which has been a convenient for simulations. This has been achieved whilst maintaining individualized cell data. The time required to run the model increases approximately linearly with time. Currently, when cell numbers exceed

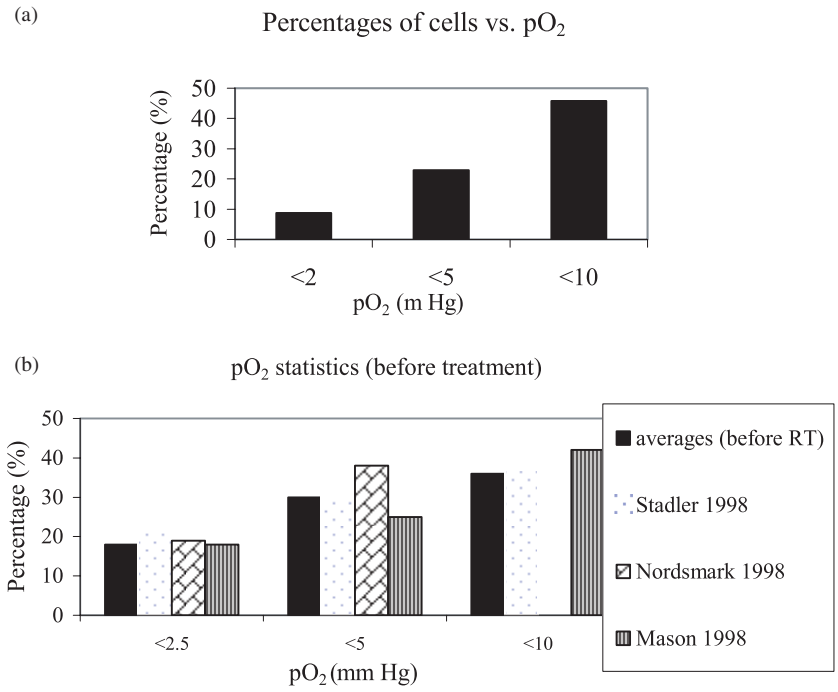

Figure 11. Percentages of cells with various pO_2 upper limits (a) from the program, (b) from literature data.

10^8, the array required for data storage becomes too large for FORTRAN 95 to handle, unless manual overrides are performed. This limitation will be looked into in the future, so that cell propagation up to approximately 10^9 cells will become possible.

3.3. Modelling hypoxia

3.3.1. The distribution of oxygen in the modelled cell population. With the use of the log normal shaped pO_2 distribution and the gradual slowing of the assigned cell cycle time according to pO_2 (linear relationship), the effect on cell quiescence of extreme hypoxia was investigated. It was found that only cells with pO_2 values less then 1–2 mm Hg could be arrested in the cell cycle, without causing tumour growth to slow too rapidly or stop completely, using the oxygen distribution in figure 4.

The percentages of cells in the very low pO_2 regions ($<$ 1 to 2 mm Hg) is approximately 5%–10%, while the percentages $<$5 mm Hg and 10 mm Hg are 25% and 50%, respectively, as shown in figure 11(a)). These figures are within the range of pO_2 values recorded in the literature from experimental studies predominantly using Eppendorf probes to measure *in vivo* oxygen tension within human HNSCC hypoxic tumours (Stadler *et al* 1998, Lartigau *et al* 1998, Nordsmark *et al* 1998, Mason *et al* 1998) shown in figure 10(b)). Literature values for these percentages often use 2.5, 5.0 or 10.0 mm Hg cut off points to define hypoxia; however, since pO_2 was assigned using integer values in the model, pO_2 values of 2, 5, 10 and 20 mm Hg were used as thresholds.

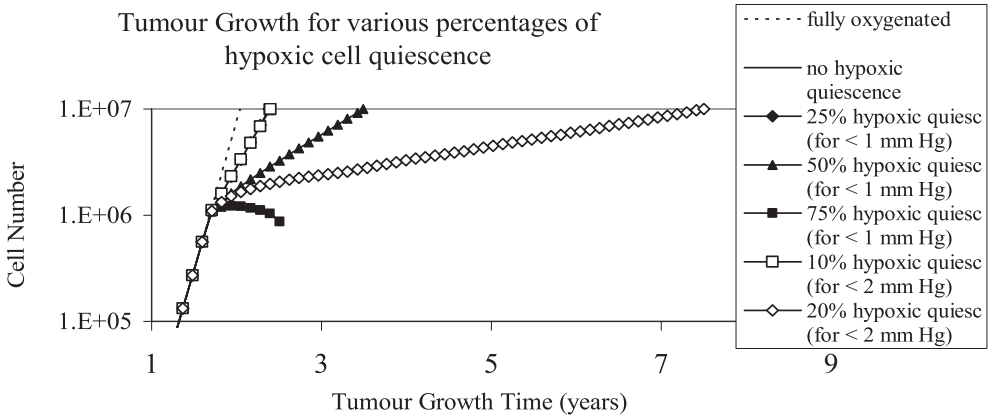

Figure 12. Tumour growth curves comparing the set probability of quiescence (full cell cycle arrest) of hypoxic cells and a quiescent hypoxic cell half life of 4 days.

3.3.2. The effects of hypoxia on tumour growth curves and doubling times. A range of quiescence probabilities was assigned to cells with extreme hypoxia (<1 or 2 mm Hg), where growth curves are shown in figure 12. The curve for 75% quiescence considering cells with $pO_2 < 1$ mm Hg is not considered plausible due to the reduction in cell numbers. It has been assumed that a tumour which has reached the point of hypoxia initiation does not reduce in cell number after this point in time. If this were the case, very few tumours would reach clinical sizes, in a hypoxic state. Based on a 50% probability of hypoxic cell quiescence for cells with a pO_2 value less than 1 mm Hg, tumour growth time increases from 2 to 3.5 years for a tumour of 10^7 cells. This probability hypoxic cell quiescence is estimated to be the most plausible, considering the effect on tumour growth after it is applied. Probability values which produce the effect of decreasing the number of tumour cells and were not considered plausible due to the prevalence of tumours that do grow to clinical sizes that exhibit hypoxia. These limits are approximately 70% if considering cell with $pO_2 < 1$ mm Hg, or 25% if considering all cell with $pO_2 < 2$ mm Hg.

If extended to a tumour consisting of 10^9 cells (using interpolation) and the same proliferative hierarchy and cell percentages, the total tumour growth time increases from 3 to 8 years. The precise value of pO_2 for which a hypoxic cell becomes quiescent is not clear from the literature. However, the level is likely to be low (0.2–1 mm Hg, Ljungkvist *et al* 2002), which is further supported by the work previously mentioned and shown is in figure 4 (Alarcon *et al* 2004). This likely low oxygen range for hypoxia induced cell quiescence, highlights the likelihood of tumour cells be subjected to relatively low oxygen pressures of 10 mm Hg or less (and consequential increase in radioresistance of 20% to 60%), whilst maintaining division capability.

With a great proportion of cells having a high probability of being quiescent, and another great proportion of cells having an oxygen level low enough to slow the cells cycle, it is reasonable to conclude that the increase in tumour doubling time in hypoxic tumours should be more than two-fold in poorly oxygenated tumours (since ∼50% of cells have a $pO_2 <$ 2.5 mm Hg in poorly oxygenated tumours, Dasu *et al* (2005)). Likely hypoxic quiescence limits and probabilities are displayed in figure 13, where a 50% quiescence probability for cells with a $pO_2 < 1$ mm Hg increases TD from 40 to 220 days. This is within the range of tumour doubling times (20–240 days) of a HNSCC patient whilst waiting for radiotherapy treatment, which includes tumours with a variety of oxygenation levels (Jensen *et al* 2007).

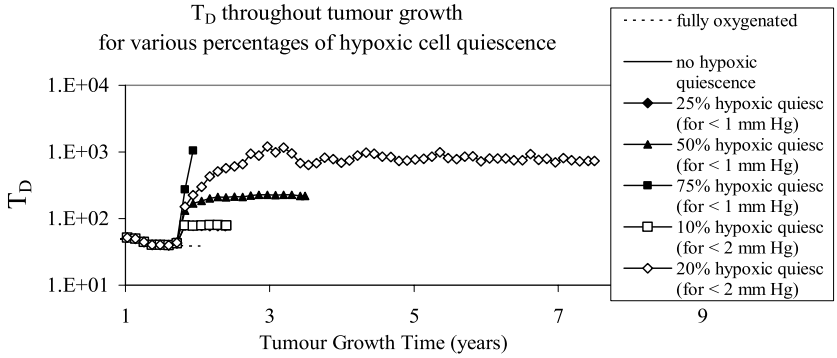

Figure 13. Tumour doubling times during growth for different probabilities of hypoxic quiescence and a hypoxic quiescent half life of 4 days. Note that the curves for 25% of cells with $pO_2 < 1$ mm Hg is very close to the curve for 10% for cells with pO2 <20 mm Hg.

Varying the quiescent hypoxic cell half life from 4 to 10 days did not make a significant change to the tumour growth rate. This is because these cells are no longer cycling and do not play a role in increasing tumour volume. The only difference between the cell population statistics for simulation which vary this parameter is the overall increasing in quiescent hypoxic cell number by 3%. However, the increase in growth time was non-significant compared to variations seen through the variation in random number seed (<20 days).

Until more quantitative data are available, future simulations will be based on a 4 day hypoxic cell half life and 50% extreme ($pO_2 < 1$ mm Hg) hypoxic cell quiescence. This, along with the log-normal pO_2 distribution used results in an approximate 20% hypoxic fraction (cells having $pO_2 < 10$ mm Hg), with 9% of cells having a pO_2 less than 2 mm Hg, and 4% of the cell population in hypoxia induced cell cycle arrest. This tumour would fall between the categories of poorly to moderately hypoxic (Dasu *et al* 2005) and is in line with the median percentage of cells (15%) below 2.5 mm Hg in from a study by Nordsmark *et al* (1996), involving 35 head and neck cancer patients.

4. Conclusions

A tumour growth model algorithm has been designed and implemented in the FORTRAN 95 programming language. It models the individual cell division of epithelial cells with a plausible cell hierarchy structure and literature researched tumour cell parameters. The algorithm is efficient in time and for memory capacity, which is achieved through an object oriented 2D cell array approach to data storage. A plausible and experimentally verified oxygen distribution has been used to randomly assign each cell a pO_2 (mm Hg) value upon entry into the cell cycle, where one daughter cells receives the mother cell pO_2 and the second daughter cell receives a random pO_2 from the distribution. The distribution is log-normal in shape which agrees well with *in vivo* data from the literature (Lartigau *et al* 1998, Adam *et al* 1999).

The stem cell population percentage dominates the rate of tumour growth for fully oxygenated simulated tumours. There is a linear relationship between the stem cell population percentage and the average tumour growth rate and an exponential relationship between stem cell population percentage and the tumour doubling time. The implementation of a realistic oxygen distribution among the tumour cells had the effect of increasing the tumour growth time and tumour doubling time. This is due to the slowing of the cell cycle for moderately

hypoxic cells and cell cycle arrest of cells under extreme hypoxia. The oxygenation attribute was applied to all cell types equally and consequently slowed the growth due to a decreased proliferation rate of stem and transit cells.

The pO_2 limit for cell quiescence had a large impact on the decrease in tumour growth rate. A plausible pO_2 value for hypoxia induced quiescence has been found to lie above 0 mm and below 2 mm Hg. Using a 50% probability for cells with a $pO_2 < 1$ mm Hg to become quiescent, the growth time was increased by 1.5 years for a 10^7 cell tumour and 5 years for a 10^9 cell tumour. The corresponding tumour doubling time increased from around 40 days to over 200 days for an oxygenated versus hypoxic tumour using this probability, which is a plausible result for a hypoxic tumour (Jensen *et al* 2007).

This study has outlined the need for specific cellular based parameters, if individualized tumour modelling is to become routine practice for radiotherapy planning. With such a large range of plausible values and distributions, such as the distribution of oxygen, it is crucial that more experimental studies be performed based on the development of relatively quick and non-invasive procedures on cancer patients prior to treatment (as well as during treatment in the cases of accelerated repopulation and reoxygenation). The lower limit for oxygen deprivation induced cell cycle arrest needs further investigation to determine if the limit differs between different cell types and tumours, as well as experimental and quantitative evidence of the degree of cell cycle time increase for moderate levels of hypoxia.

It is the intention of the authors to perform *in vivo* xenograft studies to measure and verify the pO_2 distribution within the HNSCC tumour system before and during fractionated radiotherapy. The model will also be extended to include response to radiotherapy, which can be directly compared to clinical trial data on local control outcomes from specific stratified patient groups (Nordsmark *et al* 2005, Dunst *et al* 2003, Stadler *et al* 1999). Reoxygenation dynamics and accelerated repopulation phenomenon will be key features of future versions of this tumour growth and radiotherapy model.

References

Aarnaes E *et al* 1990 Mathematical model analysis of mouse epidermal cell kinetics measured by bivariate DNA/anti-bromodeoxyuridine flow cytometry and continuous [3H]-thymidine labelling *Cell Tissue Kinet.* **23** 409–24

Aarnaes E *et al* 1993 Heterogeneity in the mouse epidermal cell cycle analysed by computer simulations *Cell Prolif.* **26** 205–19

Adam M F *et al* 1999 Tissue oxygen distribution in head and neck cancer patients *Head Neck* **21** 146–53

Adelstein D J 2005 *Squamous Cell Head and Neck Cancer* (Totowa, NJ: Humana) pp 368

Alarcon T *et al* 2004 A mathematical model of the effects of hypoxia on the cell-cycle of normal and cancer cells *J. Theor. Biol.* **229** 395–411

Appleton D R *et al* 2002 Simulation of cell proliferation in mouse oral epithelium, and the action of epidermal growth factor: evidence for a high degree of synchronization of the stem cells *Cell Prolif.* **35** 68–77 (Suppl. 1)

Becker A *et al* 1998 Oxygenation of squamous cell carcinoma of the head and neck: comparison of primary tumors, neck node metastases, and normal tissue *Int. J. Radiat. Oncol. Biol. Phys.* **42** 35–41

Begg A C *et al* 1999 The value of pretreatment cell kinetic parameters as predictors for radiotherapy outcome in head and neck cancer: a multicenter analysis *Radiother. Oncol.* **50** 13–23

Borkenstein K *et al* 2004 Modeling and computer simulations of tumor growth and tumor response to radiotherapy *Radiat. Res.* **162** 71–83

Bourhis J *et al* 2006 Phase III randomized trial of very accelerated radiation therapy compared with conventional radiation therapy in squamous cell head and neck cancer: a GORTEC trial *J. Clin. Oncol.* **24** 2873–8

Brizel D M *et al* 1999 Oxygenation of head and neck cancer: changes during radiotherapy and impact on treatment outcome *Radiother. Oncol.* **53** 113–7

Dasu A *et al* 2005 The effects of hypoxia on the theoretical modelling of tumour control probability *Acta Oncol.* **44** 563–71

Denham J W and Kron T 2001 Extinction of the weakest *Int. J. Radiat. Oncol. Biol. Phys.* **51** 807–19

Dinshaw K A *et al* 2006 Radical radiotherapy in head and neck squamous cell carcinoma: an analysis of prognostic and therapeutic factors *Clin. Oncol. (R. Coll. Radiol.)* **18** 383–9

Dionysiou D D *et al* 2004 A four-dimensional simulation model of tumour response to radiotherapy *in vivo*: parametric validation considering radiosensitivity, genetic profile and fractionation *J. Theor. Biol.* **230** 1–20

Donaghey C E 1980 CELLSIM: cell cycle simulation made easy *Int. Rev. Cytol.* **66** 171–210

Dutching W and Vogelsaenger T 1981 Three dimensional pattern generation applied to spheroidal tumor growth in a nutrient medium *Int. J. Biomed. Comput.* **12** 377–92

Dutching W and Vogelsaenger T 1985 Recent progress in modelling and simulation of three-dimensional tumor growth and treatment *Biosystems* **18** 79–91

Dunst J *et al* 2003 Tumor volume and tumor hypoxia in head and neck cancers. The amount of the hypoxic volume is important *Strahlenther. Onkol.* **179** 521–6

Durand R E and Sham E 1998 The lifetime of hypoxic human tumor cells *Int. J. Radiat. Oncol. Biol. Phys.* **42** 711–5

Elkind M *et al* 1965 Oxygen, nitrogen, recovery and radiation therapy *Cellular Radiation Biology: a Symp. Considering Radiation Effects in the Cell and Possible Implications for Cancer Therapy. a Collection of Papers Presented at the 18th Ann. Symp. on Fundamental Cancer Research* (Baltimore, MD: Lippincott, Williams and Wilkins)

Gardner L B *et al* 2001 Hypoxia inhibits G1/S transition through regulation of p27 expression *J. Biol. Chem.* **276** 7919–26

Gatenby R A *et al* 1988 Oxygen distribution in squamous cell carcinoma metastases and its relationship to outcome of radiation therapy *Int. J. Radiat. Oncol. Biol. Phys.* **14** 831–8

Gray L H *et al* 1953 The concentration of oxygen dissolved in tissues at the time of irradiation as a factor in radiotherapy *Br. J. Radiol.* **26** 638–48

Hall E J and Giaccia A J 2005 *Radiobiology for the Radiologist* (Baltimore, MD: Lippincott Williams and Wilkins)

Harting C *et al* 2007 Single-cell-based computer simulation of the oxygen-dependent tumour response to irradiation *Phys. Med. Biol.* **52** 4775–89

Henrikson *et al* 1997 *NMS Histology, Figure 5-1* (Baltimore, MD: Lippincott, Williams & Wilkins) p 49

Hill A V 1928 The diffusion of oxygen and lactic acid through tissues *Proc. R. Soc. Lon.* B **104** 39–96

Hirst D G and Denekamp J 1979 Tumour cell proliferation in relation to the vasculature *Cell Tissue Kinet.* **12** 31–42

Izquierdo J N and Gibbs S J 1972 Circadian rhythms of DNA synthesis and mitotic activity in hamster cheek pouch epithelium *Exp. Cell Res.* **71** 402–8

Jensen A R *et al* 2007 Tumor progression in waiting time for radiotherapy in head and neck cancer *Radiother. Oncol.* **84** 5–10

Kansal A R *et al* 2000 Simulated brain tumor growth dynamics using a three-dimensional cellular automaton *J. Theor. Biol.* **203** 367–82

Kirkpatrick J P *et al* 2004 Predicting the effect of temporal variations in pO_2 on tumor radiosensitivity *Int. J. Radiat. Oncol. Biol. Phys.* **59** 822–33

Kocher M *et al* 2000 Computer simulation of cytotoxic and vascular effects of radiosurgery in solid and necrotic brain metastases *Radiother. Oncol.* **54** 149–56

Koritzinsky M *et al* 2001 Cell cycle progression and radiation survival following prolonged hypoxia and re-oxygenation *Int. J. Radiat. Biol.* **77** 319–28

Koukourakis M I *et al* 2006 Endogenous markers of two separate hypoxia response pathways (hypoxia inducible factor 2 alpha and carbonic anhydrase 9) are associated with radiotherapy failure in head and neck cancer patients recruited in the CHART randomized trial *J. Clin. Oncol.* **24** 727–35

Lartigau E *et al* 1998 Variations in tumour oxygen tension (pO_2) during accelerated radiotherapy of head and neck carcinoma *Eur. J. Cancer* **34** 856–61

Leary A G *et al* 1984 Single cell origin of multilineage colonies in culture. Evidence that differentiation of multipotent progenitors and restriction of proliferative potential of monopotent progenitors are stochastic processes *J. Clin. Invest.* **74** 2193–7

Ljungkvist A S *et al* 2005 Hypoxic cell turnover in different solid tumor lines *Int. J. Radiat. Oncol. Biol. Phys.* **62** 1157–68

Ljungkvist A S *et al* 2002 Vascular architecture, hypoxia, and proliferation in first-generation xenografts of human head-and-neck squamous cell carcinomas *Int. J. Radiat. Oncol. Biol. Phys.* **54** 215–28

Mantel C *et al* 2001 Steel factor regulates cell cycle asymmetry *Stem Cells* **19** 483–91

Marcu L *et al* 2004 Modelling of post-irradiation accelerated repopulation in squamous cell carcinomas *Phys. Med. Biol.* **49** 3767–79

Marcu L *et al* 2002 Growth of a virtual tumour using probabilistic methods of cell generation *Australas. Phys. Eng. Sci. Med.* **25** 155–61

Maseide K and Rofstad E K 2000 Mathematical modeling of chronical hypoxia in tumors considering potential doubling time and hypoxic cell lifetime *Radiother. Oncol.* **54** 171–7

Mason R P *et al* 1998 Regional tumor oxygen tension: fluorine echo planar imaging of hexafluorobenzene reveals heterogeneity of dynamics *Int. J. Radiat. Oncol. Biol. Phys.* **42** 747–50

McElwain D L *et al* 1979 A model of vascular compression in solid tumors *J. Theor. Biol.* **78** 405–15

Morris R J 2004 A perspective on keratinocyte stem cells as targets for skin carcinogenesis *Differentiation* **72** 381–6

Nordsmark M *et al* 2005 Prognostic value of tumor oxygenation in 397 head and neck tumors after primary radiation therapy: an international multi-center study *Radiother. Oncol.* **77** 18–24

Nordsmark M *et al* 1996 Pretreatment oxygenation predicts radiation response in advanced squamous cell carcinoma of the head and neck *Radiother. Oncol.* **41** 31–9

Palcic B and Skarsgard L D 1984 Reduced oxygen enhancement ratio at low doses of ionizing radiation *Radiat. Res.* **100** 328–39

Potten C S 1981 The cell kinetic mechanism for radiation-induced cellular depletion of epithelial tissue based on hierarchical differences in radiosensitivity *Int. J. Radiat. Biol. Relat. Stud. Phys. Chem. Med.* **40** 217–25

Potten C S 1986 Cell cycles in cell hierarchies *Int. J. Radiat. Biol. Relat. Stud. Phys. Chem. Med.* **49** 257–78

Qi A S *et al* 1993 A cellular automaton model of cancerous growth *J. Theor. Biol.* **161** 1–12

Rischin D *et al* 2006 Prognostic significance of [18F]-misonidazole positron emission tomography-detected tumor hypoxia in patients with advanced head and neck cancer randomly assigned to chemoradiation with or without tirapazamine: a substudy of Trans-Tasman Radiation Oncology Group Study 98.02 *J. Clin. Oncol.* **24** 2098–104

Smolle J and Stettner H 1993 Computer simulation of tumour cell invasion by a stochastic growth model *J. Theor. Biol.* **160** 63–72

Stadler P *et al* 1998 Changes in tumor oxygenation during combined treatment with split-course radiotherapy and chemotherapy in patients with head and neck cancer *Radiother. Oncol* **48** 157–64

Stadler P *et al* 1999 Influence of the hypoxic subvolume on the survival of patients with head and neck cancer *Int. J. Radiat. Oncol. Biol. Phys.* **44** 749–54

Steel G G 1997 *Basic Clinical Radiobiology* 2nd edn (London: Edward Arnold)

Steel G 2002 *Basic Clinical Radiobiology* 3rd edn (London: Edward Arnold)

Tannock I F 1968 The relation between cell proliferation and the vascular system in a transplanted mouse mammary tumor *Br. J. Cancer* **22** 258–73

Tannock I F 1972 Oxygen diffusion and the distribution of cellular radiosensitivity in tumors *Br. J. Radiol.* **45** 515–24

Tannock I F and Steel G G 1970 Tumor growth and cell kinetics in chronically hypoxic animals *J. Natl. Cancer Inst.* **45** 123–33

Tannock I and Hill R 1998 *The Basic Science of Oncology* 3rd edn (New York: McGraw-Hill)

Thomlinson R H and Gray L H 1955 The histological structure of some human lung cancers and the possible implications for radiotherapy *Br. J. Cancer* **9** 539–49

Webster L *et al* 1998 Cell cycle distribution of hypoxia and progression of hypoxic tumour cells *in vivo Br. J. Cancer* **77** 227–34

Wilson G D *et al* 1995 Studies with bromodeoxyuridine in head and neck cancer and accelerated radiotherapy *Radiother. Oncol.* **36** 189–97

Wilson G D *et al* 1988 Measurement of cell kinetics in human tumours *in vivo* using bromodeoxyuridine incorporation and flow cytometry *Br. J. Cancer* **58** 423–31

Wright E A and Howard-Flanders P 1957 The influence of oxygen on the radiosensitivity of mammalian tissues *Acta radiol* **48** 26–32

Wright N and Alison M 1984 *The Biology of Epithelial Cell Populations* vol 1 (Oxford: Clarendon)